J. Fluid Mech. (1989), *vol.* 202, *pp.* 1–16
Printed in Great Britain

Frontogenesis in a fluid with horizontal density gradients

By J. E. SIMPSON AND P. F. LINDEN
Department of Applied Mathematics and Theoretical Physics, University of Cambridge, Silver Street, Cambridge, CB3 9EW, UK

(Received 29 January 1987 and in revised form 15 July 1988)

The adjustment under gravity of a fluid containing a horizontal density gradient is described. The fluid is initially at rest and the resulting motion is calculated as the flow accelerates, driven by the baroclinic density field. Two forms of the initial density distribution are considered. In the first the initial horizontal gradient is constant. A purely horizontal motion develops as the isopycnals rotate towards the horizontal. The vertical density gradient increases continually with time but the horizontal density gradient remains unchanged. The horizontal velocity has a uniform vertical shear, and the gradient Richardson number is constant in space and decreases monotonically with time to $\frac{1}{2}$. The second density distribution consists of a piecewise constant gradient with a jump in the gradient along a vertical isopycnal. The density is continuous. In this case frontogenesis is predicted to occur on the isopycnal between the two constant-density-gradient regions, and the timescale for the formation of a front is determined. Laboratory experiments are reported which confirm the results of these calculations. In addition, lock exchange experiments have been carried out in which the horizontal mean gradient is represented by a series of step density differences separated by vertical gates.

1. Introduction

When a horizontal density gradient exists in a fluid in the presence of a vertical gravitational field vorticity is generated and flow is induced no matter how small the density gradient. The resulting motion advects fluid particles and the density gradient may either be increased or decreased. In the extreme case, the density gradient may increase to such an extent that an effective discontinuity or front may develop.

Fronts in stratified fluids are regions where mixing is observed to occur (Simpson 1982). This is an irreversible process and so once frontogenesis has occurred the motion undergoes a fundamental change. In this paper we describe some simple calculations of the motion produced by a horizontal density gradient. These calculations show under what conditions frontogenesis will occur and we describe a set of laboratory experiments to test these conclusions.

The direct motivation for the present work arose from a desire to understand the observations we have recently made in some laboratory experiments (Linden & Simpson 1986 hereinafter referred to as LS) on the effects of turbulence on gravity currents. In LS a gravity current was produced by lock exchange in water kept turbulent by bubbling air through it. As the gravity current travelled along it was continually mixed by the bubbles until eventually all the vertical stratification was removed. There still remained a horizontal density gradient associated with the

original density difference on the two sides of the lock and this drove a mean gravitational circulation in the tank. If the turbulence was maintained the eventual state was a completely uniform density in the tank.

On the other hand, if the bubbles were turned off while there was still a horizontal density gradient a horizontal counterflow was observed with fluid from the dense end of the tank flowing underneath the lighter fluid coming from the other end of the tank. A vertical stratification was re-established as the flow accelerated. More importantly, frontogenesis was found to occur with the sharpening up of the horizontal density gradient as the fluid moved along the tank. Eventually, a gravity-current-type head was produced with the typical sharp front and breaking Kelvin–Helmholtz billows at the rear (Simpson & Britter 1979).

This observation raises the question of what causes this frontogenesis. In LS it was suggested, partly with the aid of hindsight of the work described below, that the frontogenesis was associated with *non-uniformities* in the horizontal density gradient. In that experiment the nonlinearities (or non-uniformities) are associated with the zero-flux boundary conditions associated with the solid endwalls of the tank, which imply that $\rho_x = 0$ at the ends. Here ρ is the fluid density and x is measured along the length of the tank. Using values of the density difference between the ends of the tank, LS found fair agreement between calculated and observed travel times for the front.

The LS experiment is not a particularly clean one for investigating frontogenesis. The horizontal density gradient cannot conveniently be set *a priori*, and the origin of time is poorly defined as it is necessary to wait until the turbulence decays. As a result we have carried out a series of experiments in which the horizontal density gradient can be established precisely and the fluid released from rest. In this way different forms of the horizontal density variation can be set up and the ensuing motion of the fluid studied. The outline of the paper is as follows. In §2 some theoretical calculations of the motion in an unbounded fluid with a constant density gradient are given. These show that a horizontal flow with vertical shear is established and that at large times the gradient Richardson number approaches $\frac{1}{2}$. It is shown that frontogenesis does not occur unless there are non-uniformities in the density gradient and the evolution of a piecewise constant density gradient is calculated in §3. The experiments are described in §4 and the results discussed in §5. A step analogue of the horizontal gradient experiment is described in §6 and the conclusions given in §7.

2. Evolution of a constant density gradient

In this section we examine the motion of an unbounded fluid released from rest with *uniform* initial gradients of density in the horizontal and vertical. We include the possibility of an initial stable, vertical density gradient for generality and also because this conforms to the laboratory experiments described in §4.

We consider two dimensional motion in the (x, z)-plane, with Ox horizontal and Oz antiparallel to gravity $\boldsymbol{g}$. The fluid is initially at rest so that $\boldsymbol{u} = (u, w) = (0, 0)$ and the initial density is given by

$$\rho = \bar{\rho}(1-\alpha x-\beta z), \quad \alpha > 0, \beta > 0. \tag{2.1}$$

We choose $\alpha > 0$ so that the fluid is heavy to the left (as in the case in the experiments) and $\beta > 0$ to ensure static stability (see figure 1). The initial value of θ, the angle the isopycnals make with the vertical is given by $\tan\theta = \beta/\alpha$.

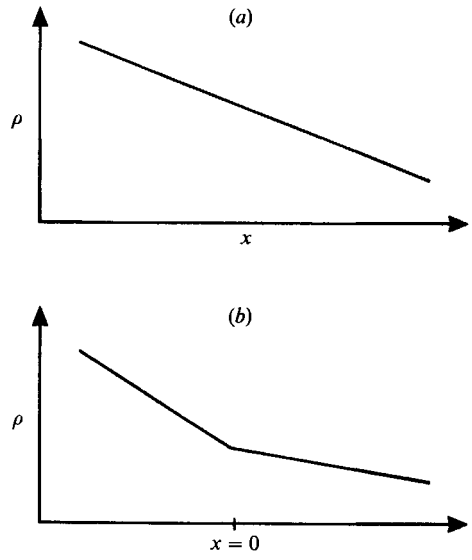

FIGURE 1. The initial horizontal density variation: (*a*) constant density gradient; (*b*) piecewise constant gradient with continuous density distribution.

The equations governing the Boussinesq, inviscid flow with no further approximation but under the assumption that $w = 0$, are

$$\bar{\rho} u_t = -p_x, \tag{2.2}$$

$$g\rho = -p_z, \tag{2.3}$$

$$\rho_t = -u\rho_x, \tag{2.4}$$

$$u_x = 0. \tag{2.5}$$

The pressure p is eliminated from (2.1) using the hydrostatic relation (2.3). Differentiation of the resulting equation with respect to x and the use of continuity (2.5) shows that

$$\rho_{xx} = 0. \tag{2.6}$$

This is a necessary condition for the solution of (2.1)–(2.5) showing that frontogenesis is associated with the presence of a vertical velocity and transverse circulation.

In the restricted case where the horizontal density gradient $-\alpha\bar{\rho}$ is constant a solution to the full problem can be found. It is easily seen that this solution is

$$\left.\begin{aligned} u &= -g\alpha z t, \\ \rho &= \bar{\rho}(1-\alpha x-\beta z)-\tfrac{1}{2}g\bar{\rho}\,\alpha^2 z t^2. \end{aligned}\right\} \tag{2.7}$$

Thus a uniform vertical shear flow is established which accelerates at a constant rate. The horizontal density gradient remains at its original value $-\alpha\bar{\rho}$ while the vertical stratification continually increases in strength. The isopycnals rotate towards the horizontal with

$$\tan\theta = \beta/\alpha + \tfrac{1}{2}g\alpha t^2. \tag{2.8}$$

A measure of the stability of the flow is provided by the gradient Richardson number $Ri = -g\rho_z/\bar{\rho}u_z^2$. From (2.7) we see that

$$Ri = \tfrac{1}{2} + \beta/g\alpha^2 t^2. \tag{2.9}$$

The Richardson number decreases with time (at the initial instant it is infinite) and approaches $\frac{1}{2}$ as $t \to \infty$. This result suggests that the flow will be linearly stable.

It is interesting to note that the solution (2.7) also satisfies the viscous equations of motion and in the absence of boundaries viscosity does not alter the solution. In the experiments to be described below boundary layers form on the top and bottom surfaces of the tank. However, we shall see that their influence is weak and that they are suppressed by the vertical density stratification.

3. Frontogenesis

The results of the previous section show that frontogenesis does not occur when the initial horizontal density gradient is constant. For non-uniform density gradients it is necessary to include the vertical motion and so the governing equations are

$$\bar{\rho}(u_t + uu_x + wu_z) = -p_x, \tag{3.1}$$

$$\bar{\rho}(w_t + uw_x + ww_z) = -p_z - g\rho, \tag{3.2}$$

$$\rho_t + u\rho_x + w\rho_z = 0, \tag{3.3}$$

$$u_x + w_z = 0. \tag{3.4}$$

Using (3.4) we define a stream function $\psi(x, z)$ by

$$u = -\psi_z, \quad w = \psi_x. \tag{3.5}$$

We consider the time evolution of this system by writing the solution as a power series in time t:

$$\left.\begin{aligned} \psi &= \psi_0 + \psi_1 t + \psi_2 t^2 + \ldots, \\ \rho &= \rho_0 + \rho_1 t + \rho_2 t^2 + \ldots, \end{aligned}\right\} \tag{3.6}$$

Since the fluid is at rest initially, $\psi_0 = 0$ and $\rho_0 = \rho_0(x, z)$ is the initially specified density distribution. We substitute (3.6) into (3.1)–(3.5), eliminate the pressure from (3.1) and (3.2) and equate the coefficients of the power series in t.

At $O(1)$ we have

$$\nabla^2 \psi_1 = -\frac{g\rho_{0x}}{\bar{\rho}}, \tag{3.7}$$

and

$$\rho_1 = 0. \tag{3.8}$$

Differentiation of (3.7) gives

$$\nabla^2 w_1 = -\frac{g}{\bar{\rho}}\rho_{0xx}, \quad \nabla^2 u_1 = \frac{g}{\bar{\rho}}\rho_{0xz}. \tag{3.9}$$

This shows how the vertical velocity is associated with the *curvature* in the horizontal density distribution. From (3.8) we see that the derivative of (3.3) may be approximated by

$$\rho_{xt} = -(u\rho_x)_x \tag{3.10}$$

and so the time evolution of the density gradient is determined by the sign of $(u\rho_x)_x$. This implies that an increase in the horizontal density gradient, and ultimately frontogenesis, will only occur when the horizontal motion in the region of stronger density gradient is towards the region of the weaker density gradient.

In order to make detailed comparisons with our laboratory experiments, we shall treat the case where the initial density gradient is piecewise constant and is given by

$$\begin{aligned} \rho &= \bar{\rho}(1-\alpha_1 x), \quad x < 0, \\ &= \bar{\rho}(1-\alpha_2 x), \quad x > 0. \end{aligned} \tag{3.11}$$

There is a discontinuity in the density gradient at $x = 0$ but the density is continuous there.

Substituting (3.11) into (3.7) we have

$$\nabla^2 \psi_1 = \begin{cases} g\alpha_1, & x < 0, \\ g\alpha_2, & x > 0. \end{cases} \tag{3.12}$$

The solution in a channel with ψ = constant on $z = \pm \frac{1}{2}h$ is

$$\psi_1 = \begin{cases} \frac{1}{2}g\alpha_1 z^2 + \frac{1}{8}g\alpha_2 h^2 + 2g\dfrac{(\alpha_1-\alpha_2)h^2}{\pi^3} \displaystyle\sum_{m=0}^{\infty} \frac{(-1)^m}{(2m+1)^3} \cos\frac{(2m+1)\pi z}{h} \exp\left[\frac{(2m+1)\pi x}{h}\right], \\ \qquad\qquad x < 0, \\ \frac{1}{2}g\alpha_2 z^2 + \frac{1}{8}g\alpha_1 h^2 - 2g\dfrac{(\alpha_1-\alpha_2)h^2}{\pi^3} \displaystyle\sum_{m=0}^{\infty} \frac{(-1)^m}{(2m+1)^3} \cos\frac{(2m+1)\pi z}{h} \exp\left[\frac{-(2m+1)\pi x}{h}\right], \\ \qquad\qquad x > 0. \end{cases} \tag{3.13}$$

If the horizontal density gradients are the same for $x < 0$ and $x > 0$ ($\alpha_1 = \alpha_2$) we see that $w_1 = 0$ and $u_1 = -g\alpha z$ as found in §2 (see (2.7)). The effect of the discontinuity in the density gradient (but not in density) is to produce the additional circulation expressed as the sums in (3.13). The horizontal velocity is positive in the lower half of the tank ($z < 0$) and, if $\alpha_1 > \alpha_2$, is greater for $x < 0$ than for $x > 0$. This is a result of the steeper density gradient in the left-hand end of the tank. Mass conservation implies that the excess flux arriving at $x = 0$ from $x < 0$ must result in an upward velocity as is the case in (3.13). This upward velocity provides the mass flux towards $x = -\infty$ required in the upper half of the tank. If $\alpha_2 > \alpha_1$ the sense of the circulation is reversed.

Instantaneous streamlines for the flow with $\alpha_1 > \alpha_2$ are shown on figure 2. The streamlines are closer together on the left ($x < 0$) than on the right ($x > 0$) as a result of the more intense flow produced by the larger density gradient there. Away from $x = 0$ the solution approaches that of uniform shear as expected from the calculation of §2. A sequence showing the time evolution of the density field (calculated in the Appendix) is shown on figure 3. This shows the crowding together of the isopycnals at the lower boundary, reflecting the increase in density gradient and incipient frontogenesis there. Note also that the isopycnals no longer remain straight and curvature develops near $x = 0$. At the upper boundary the horizontal density gradient decreases with time. While it should be noted that the small-time expansion is unlikely to give accurate results for $t = 1$, the essential features of the flow are contained in this solution. An accurate solution requires nonlinear effects to be incorporated.

Far from $x = 0$ the motion is determined by the local density gradient and since the original density is advected by this motion, the timescale for an increase in the density gradient is, on dimensional grounds

$$t = c[g(\alpha_1 - \alpha_2)]^{-\frac{1}{2}}, \tag{3.14}$$

where c is an $O(1)$ constant. One aim of the experiments to be described below is to

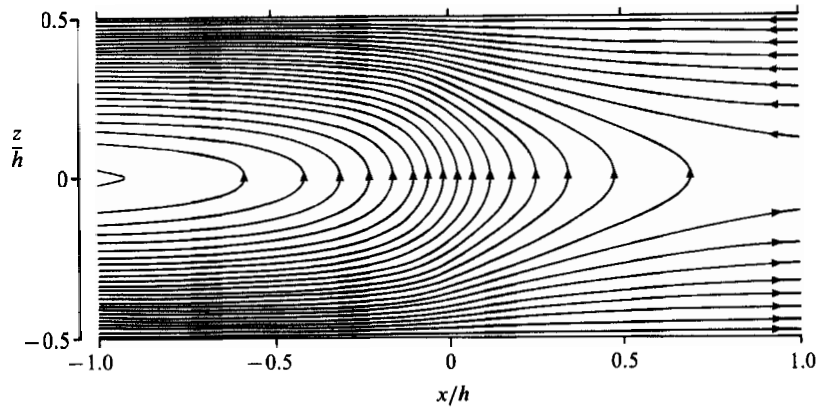

FIGURE 2. Instantaneous streamlines for the flow given by (3.13) set up by the piecewise continuous density gradient shown in figure 1 (*b*). In this case $\alpha_1 = 1.10^{-2}$ mm^{-1} and $\alpha_2 = 3.10^{-3}$ mm^{-1} and the channel depth $h = 150$ mm.

confirm this dependence and to evaluate the constant c experimentally. A similar expression for this timescale is derived from the time-series expansion and the details are given in the Appendix.

4. The experiments

The experiments were carried out in a closed rectangular tank measuring 3.6 m long, 150 mm deep and 80 mm wide. The sides of the tank were made of perspex to allow for flow visualization. The tank was mounted on a frame and pivoted about its centre so that it could be rotated from a vertical to a horizontal position (see figure 4).

Since it is clearly impossible to set up a horizontal density gradient in a fluid at rest, the tank was filled while in the vertical position. The tank was then rapidly rotated through 90° and in this way the desired horizontal density gradient was established. We discuss the motion induced by the tank rotation below, but first we describe the experimental procedure.

In the first set of experiments the tank was filled with a linear density stratification using the standard 'double bucket' technique (Oster 1965). During the filling process a small amount of dye was added to the supply at regular intervals to mark isopycnal surfaces. After rotation of the tank photographs were taken of the positions of these dye lines at subsequent stages during the motion and the observations recorded below are taken from the photographic record.

In the second series of experiments a piecewise linear density variation was established within the tank. A given density gradient was set up by the Oster method over one-half of the length of the tank. Additional salt was then added to one of the filling buckets so that a larger density gradient was set up in the other half of the tank, but the density was continuous at the division between the two gradient regions.

Once the tank had been filled and all transient motions associated with the filling process had decayed, the tank was rapidly rotated to the horizontal position and brought to rest against a stop covered with sponge rubber to absorb some of the impact. The time taken for the rotation was 2 s, which was always much less than the buoyancy period of the stratification $2\pi/N \geqslant 10$ s.

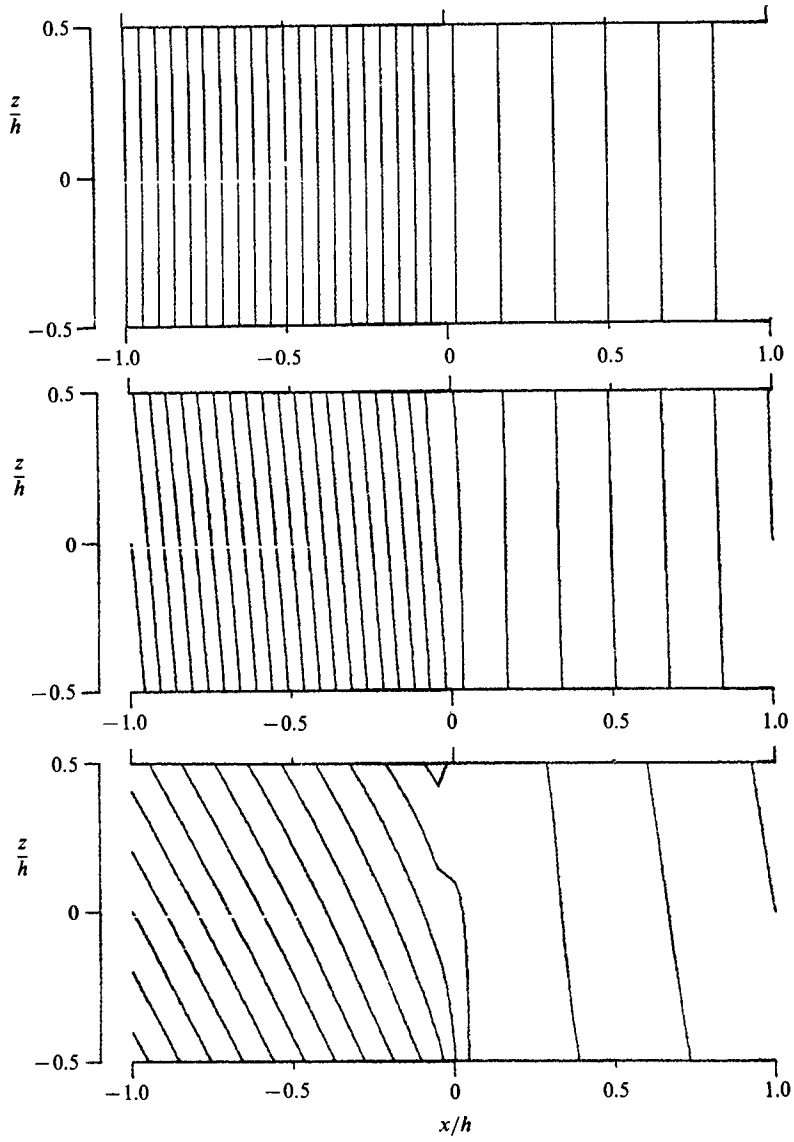

FIGURE 3. Isopycnals during the evolution of the density field calculated from (A 3), for the same conditions as in figure 2. The surfaces are drawn at the dimensionless times $\hat{t} = 0$, 0.4 and 1.0, respectively, where $\hat{t} = (g\alpha_1)^{\frac{1}{2}}t$.

The initial response of the fluid within the tank is, to an adequate approximation, the same as that for an unstratified fluid. If the fluid were to remain at rest relative to the tank during the rotation then it would have to acquire the vorticity associated with the solid-body rotation. It is clearly impossible for the vorticity to be imparted to the interior of the tank over such a short timescale and so the fluid undergoes an irrotational displacement with respect to the tank. This displacement rotates the isopycnals from the vertical, and apart from some residuals of vortex sheets generated at the walls, the fluid within the tank is instantaneously at rest when the tank rotation stops. Buoyancy forces subsequently generate motion within the tank.

The initial displacement of the isopycnals can be determined using potential flow

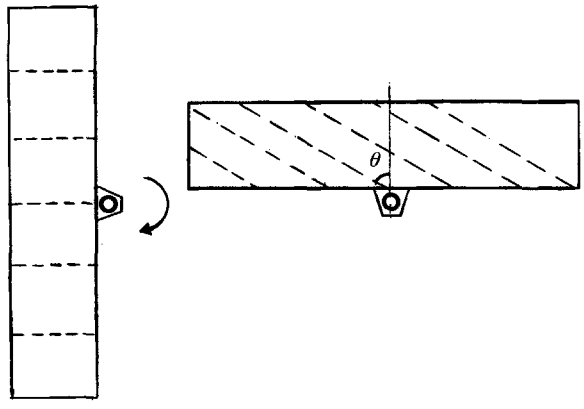

FIGURE 4. A sketch of the experimental tank showing the method for producing a horizontal density gradient as the tank is rotated through 90°. The broken lines correspond to the dyed isopycnals shown in figures 5 and 9.

theory. For the case of a rectangular prism the solution for the stream function is given in Milne-Thompson (1962, p. 271) as an infinite sum. A more convenient closed form can be obtained by considering the tank as a long ellipse of semi-major axis a and semi-minor axis b. In this case (Lamb 1932) the stream function $\psi(x, z)$ relative to the tank is

$$\psi = \omega\left(\frac{1}{a^2}+\frac{1}{b^2}\right)\left(\frac{x^2}{a^2}+\frac{z^2}{b^2}-1\right), \tag{4.1}$$

where ω is the angular velocity of the rotation.

Away from the ends of the tank the motion may be represented by an ellipse with semi-major axis $a \to \infty$. Then the velocity components are

$$u = 2\omega z, \quad v = 0. \tag{4.2}$$

The isopycnals are displaced in the direction along the tank and the total displacement

$$x = \int u\,\mathrm{d}t = 2z\int \omega\,\mathrm{d}t = \pi z, \tag{4.3}$$

when the tank is rotated through $\Phi = \int \omega\,\mathrm{d}t = \frac{1}{2}\pi$. This implies that during the motion the isopycnals remain straight and are rotated through an angle

$$\theta = +\tan^{-1}\pi. \tag{4.4}$$

A total of 19 experiments were carried out and the parameter values are shown on table 1.

5. The experimental results

5.1. *Uniform density gradient*

We first describe the flow generated by a uniform horizontal density gradient (figure 1*a*). An example of the flow generated in this case is shown on figure 5 which shows a time sequence of photographs of the flow. The times of the photographs are 8.0, 12.3, 16.7, 20.9 and 24.6 s from the moment the tank comes to rest after rotation from the vertical. The vorticity generated by the horizontal density gradient produces a flow towards the right in the lower half of the tank and towards the left in the upper

Expt no.	$\alpha_1 \times 10^5$ cm^{-1}	$\alpha_2 \times 10^5$ cm^{-1}	$2\pi/N$ s
1	6.5		24.9
2	12.1		18.1
3	13.2		17.5
4	10.6		19.5
5	18.8		14.6
6	30.0		11.6
7	3.1		36.3
8	15.0		16.4
9	5.0		28.4
10	10.3		19.8
11	7.2	5.0	23.6
12	20.0	3.3	14.2
13	8.9	2.8	21.3
14	35.5	8.3	10.6
15	17.8	13.3	15.0
16	25.0	13.3	12.7
17	19.4	13.8	14.4
18	19.4	13.3	14.4
19	30.0	13.3	11.6

TABLE 1. The experimental parameters. For experiments 1–10 a constant density gradient was established throughout the tank and $\alpha_1 = \alpha_2$

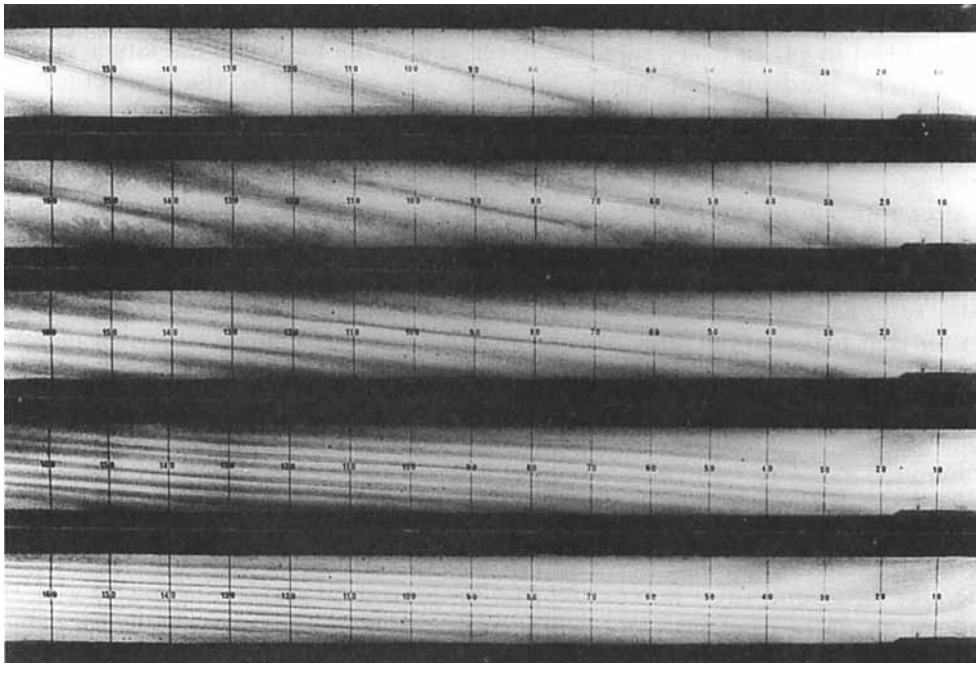

FIGURE 5. A time-sequence showing the motion of the isopycnals in experiment 8. The photographs are taken at 8.0, 12.3, 16.7, 20.9 and 24.9 s after the rotation of the tank. Only the right-hand half of the tank is visible, and the vertical lines are at 10 cm intervals measured from the right-hand end of the tank. Instabilities associated with the boundary layers on the top and bottom of the tank are visible on the first two photographs, but these are subsequently suppressed as the vertical stratification increases at later times. Otherwise, apart from the reflection at the right-hand end, the isopycnals remain straight throughout the motion.

half. This is as expected since the experiments reproduce the theoretical conditions discussed in §2 with the density increasing to the left. In these photographs the vertical lines mark 10 cm intervals from the right-hand end of the tank and only the right-hand half of the tank is visible.

The qualitative features of the flow shown in figure 5 are in agreement with the corresponding theoretical predictions in §2. The isopycnals marked with dye remain straight as they rotate towards the horizontal. There is evidence in the early stages of instabilities generated by the boundary layers on the top and bottom of the tank. These instabilities, which are clearly visible in the second panel of figure 5, are suppressed at the later times as the vertical stratification increases. Apart from the disturbance produced by reflection at the end of the channel there is no evidence of internal instabilities. The isopycnals become closer together as they rotate towards the horizontal, but there is no differential convergence which would lead to frontogenesis. Similarly there was no evidence of frontogenesis in any of the ten experiments with a constant density gradient.

The angle of inclination θ of the isopycnals to the vertical for six experiments is plotted as a function of time t on figure 6. In this log–log plot the time has been non-dimensionalized by $[\frac{1}{2}g\alpha]^{\frac{1}{2}}$, where $\alpha = (1/\bar{\rho})(\partial\rho/\partial x)$ is a measure of the horizontal density gradient. The broken line has a slope of 2 and passes through (1, 1) as suggested by (2.8). The initial angle of inclination $\tan\theta = \pi$ as given by (4.4) is also shown on this figure. We see that the data confirm very well to the theoretical predictions.

5.2. *Piecewise constant density gradient*

In experiments 11–19 a piecewise constant density gradient was set up in the tank as described in §4. In every case, the lower half of the tank had the larger value of the density gradient and when the tank was rotated to the horizontal this corresponded to the left-hand end of the tank. In the notation of §3 with $x = 0$ corresponding to the middle section of the tank, $\alpha_1 > \alpha_2$ in (3.11), as was taken to be the case.

After rotation of the tank the isopycnals were observed to tilt over in a similar manner to that observed in the case of a constant density gradient. The rate of tilt of isopycnals that were away from the central portion of the tank was observed to be the same as that for the constant-density-gradient case with the appropriate value of α for that region of the tank. This result is indicated on figure 7 where the distance x of the point of intersection of an isopycnal with the base of the tank measured from the centre of the tank ($x = 0$) is plotted against t^2 for two isopycnals, one from the stronger-gradient region ($\alpha = \alpha_1$) and the other from the weaker-gradient region ($\alpha = \alpha_2$). The value of x is related to the angle of inclination by the relation $x = x_0 + \frac{1}{2}h\tan\theta$, where h is the depth (150 mm) and x_0 the original position of the isopycnals at mid-depth. The curves shown are theoretical, based on (2.7) with the appropriate values of α in each case.

On the basis of (3.13) it is expected that for horizontal scales comparable with the tank depth, the rate of tilt will be intermediate between these two extreme values. Also plotted on figure 7 as circles are the values of x for the isopycnal originally at the junction between the two gradient regions. The rate of tilt initially follows that of the region of stronger gradient but subsequently this decreases to a value appropriate to the region of weaker density gradient. This transition to a slower rate of tilting is accompanied by visual observations of a sharpening of the density gradient (see figure 9).

In an attempt to compare the observations of increasing horizontal density

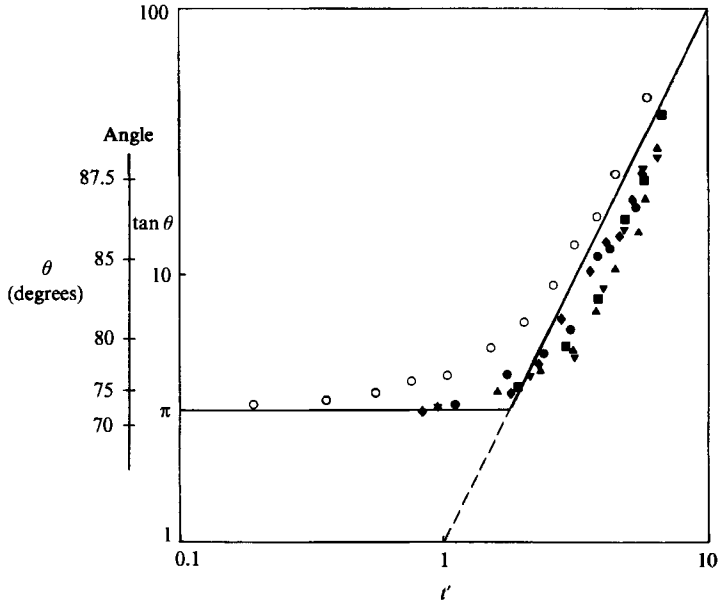

FIGURE 6. A log–log plot of the angle θ of inclination of the isopycnals to the vertical against the dimensionless time $t' = (\frac{1}{2}g\alpha)^{\frac{1}{2}}t$. The six experiments shown are those in which the initial density gradient is uniform. The lines are those predicted by the calculation in §2 and are discussed in the text.

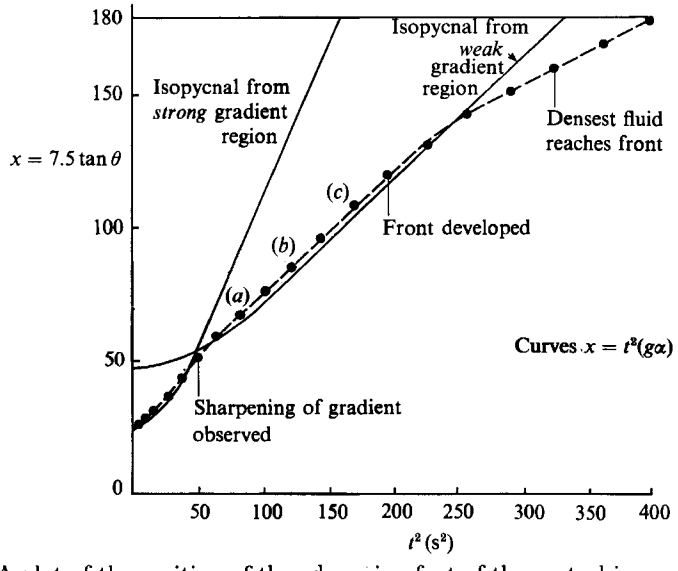

FIGURE 7. A plot of the position of the advancing foot of the central isopycnal in experiment 19, immediately after the tank reached the horizontal (●--●). The points (*a*), (*b*) and (*c*) correspond to the photographs shown in figure 9. The two solid lines show the different theoretical curves for the advance of the isopycnals in the regions of strong and weak density gradients.

gradient with the calculations in §4, the photographic records of runs 11–19 were analysed to determine the time t_c at which curvature was first observed in the isopycnals. This time can then be compared with the predicted time (3.14). A straight edge was placed along the central isopycnal and times at which significant deviation was discernable were noted. This was continued back in time through the

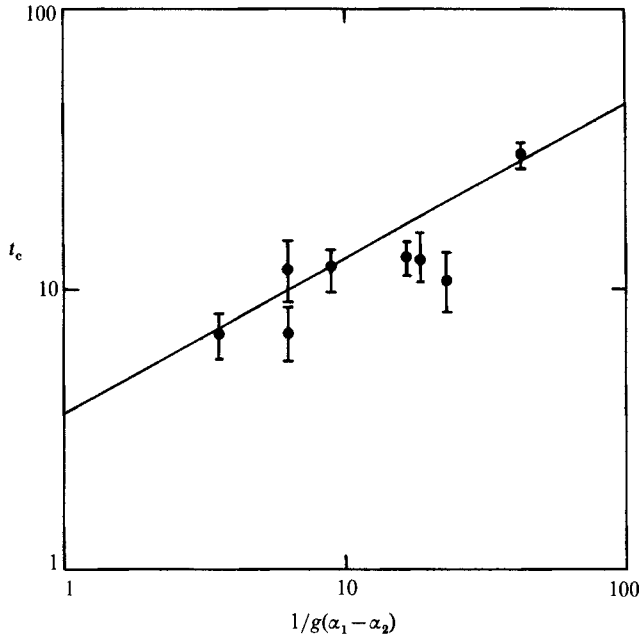

FIGURE 8. A log–log plot of the time t_c(s) for significant curvature of the isopycnals to be observed against $[g(\alpha_1-\alpha_2)]^{-1}$. The straight line has a slope of $\frac{1}{2}$ as suggested by (3.14) and is a best fit to the data. The error bars result from uncertainties in determining the onset of curvature.

photographs until we could no longer identify deviation from a straight line with any certainty. The time of the first photograph (usually taken at 1 s intervals) after this one was taken to be t_c. This is a somewhat subjective process and there is considerable uncertainty in the estimation of t_c.

The results of this analysis are shown on figure 8 where the observed time t_c is plotted against $[g(\alpha_1-\alpha_2)]^{-1}$ on a log–log plot. The straight line on the graph has a scope of $\frac{1}{2}$ as suggested by (3.14). There are rather few data points and considerable scatter but there is some measure of agreement. The data shown on figure 8 give the value of the constant c in (3.14) as $c = 4.0 \pm 1.2$.

In four of these experiments (12, 14, 16 and 19) complete frontogenesis in the formation of a gravity-current head was observed. An example from experiment 19 is shown on figure 9. The photographs show close-ups of the lower half of the tank and are taken at 9, 11 and 13 s after the tank has come to rest. Figure 5 can be used to orient these photographs within the tank as the numbers marking the vertical lines appear in both.

In the first panel a 'nose' has formed and the shadowgraph image clearly shows that a sharp density front (at 114 cm) has formed. Behind the nose the presence of fine structure on the shadowgraph is evidence of mixing and there is an enhanced vertical stratification further behind. All these features are characteristics of a classical gravity-current head (Simpson 1982). As the nose travels to the right it can be seen to catch up to the next dyed isopycnal ahead of it. This is clear evidence that the horizontal density gradient at the nose is increasing and frontogenetic processes are continuing.

The front is observed to form along the isopycnal between the two regions of constant density gradient. The initial stage of frontogenesis is the development of

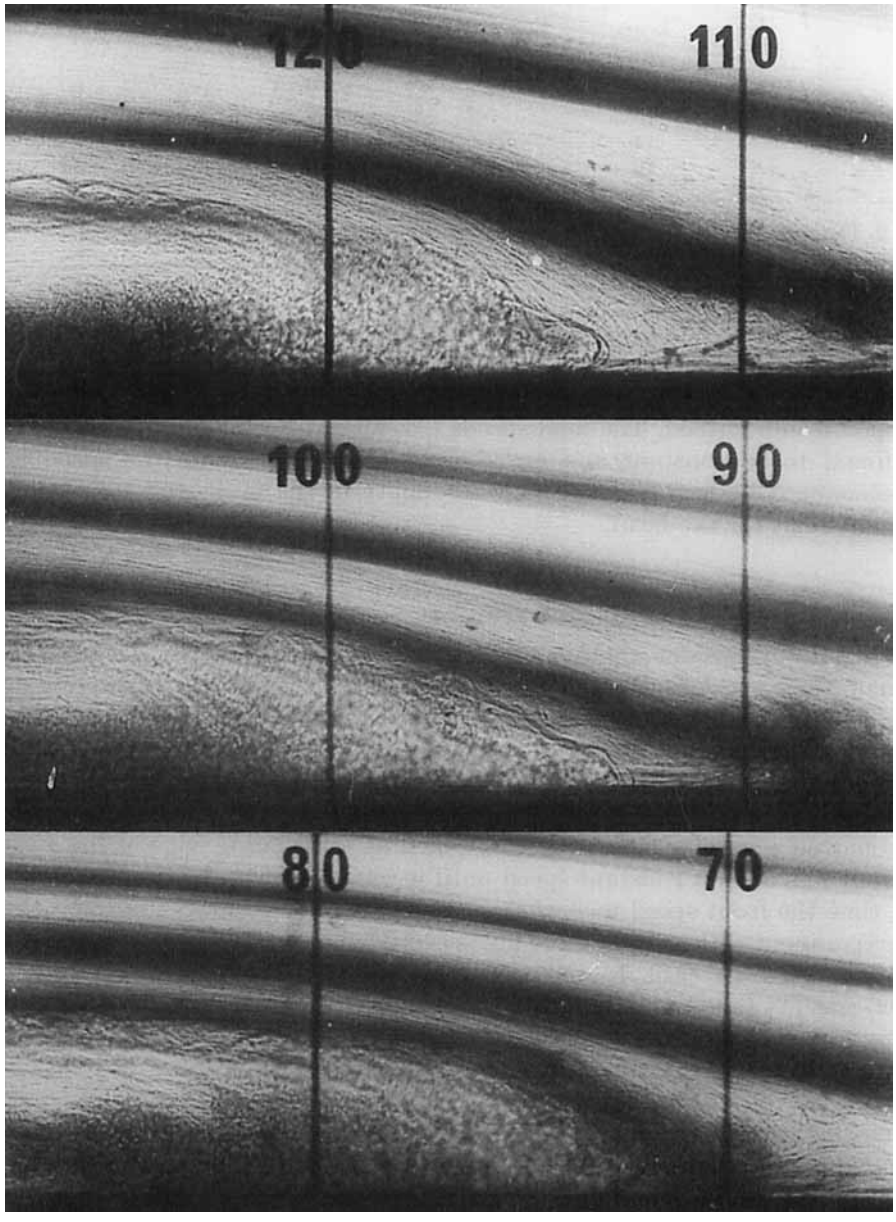

FIGURE 9. Stages during the frontogenesis observed in experiment 19. The photographs were taken at 9.0, 11.0 and 13.0 s after the tank reached the horizontal. The lower half of the tank is shown, in which the flow is from left to right. The vertical lines also appear in figure 5. Further information on this flow is shown on figure 7.

curvature in the dyeline marking that isopycnal as was discussed. That early stage is not shown on figure 9, but curvature of the adjacent isopycnal is visible in the first panel. Provided the difference in density gradients in the two halves of the tank is large enough a strong front of this nature was observed. In the other cases, although curvature of the density surfaces was detected a strong front with gravity-current structure did not form before the flow was influenced by the ends of the tank. We

Expt no.	Front speed U cm s^{-1}	Froude no. $U/(g'H)^{\frac{1}{2}}$
12	8.8	0.39
13	5.7	0.40
14	11.9	0.33
16	9.8	0.38
19	10.5	0.37

TABLE 2. The velocity U of the head in those experiments in which a fully developed front formed

believe that these flows too would eventually have produced gravity-current structures had the experimental tank been longer.

These features were observed in each of the five experiments in which fully developed fronts formed. The final speeds U achieved by the gravity-current heads were found to be constant and are shown on table 2, where the speed is non-dimensionalized by $(g'H)^{\frac{1}{2}}$, where H is the depth of the tank, and so is given as a Froude number for the head.

6. Step analogue of continuous gradient

It is helpful to consider whether a front can be formed by releasing a series of locks in each of which the density is successively reduced. This problem, of discrete-density steps, has been addressed by Nof (1979) and serves as a useful analogue of a continuous density gradient.

Two experiments were carried out. In the first with two steps, lock gates initially separated two fluids of 2% and 1% density excess over fresh water. When the gates were removed a gravity-current front formed at the leading edge of the 1% fluid. This front moved at a constant speed until it was caught up by the 2% fluid, after which time the front speed increased.

An experiment with at least three fluids is needed to produce a clear analogy of the continuous gradient case. In the second experiment three fluids, 3% (red), 2% (yellow) and 1% (blue) were simultaneously released (see figure 10, plate 1). We have now, by analogy with the continuous gradient case, a gradient reducing by three equal steps and then remaining at a fixed density (the fresh water beyond the first dense fluid).

When this experiment was run the yellow fluid began to catch up the blue, since $\mathrm{d}\rho/\mathrm{d}x = 0$ ahead of the blue, and so the fluid ahead is at rest. This is in agreement with Nof's results and our continuous-gradient experiments. During this stage, however, the red does not catch up the yellow. This region corresponds to the continuous-gradient experiment with $\mathrm{d}\rho/\mathrm{d}x$ constant and, consistent with that, there is no tendency for frontogenesis in this part of the flow. No front appears here. Finally, after the yellow fluid reaches the blue, the red fluid begins to catch up and eventually reaches, and strengthens, the front. These stages are illustrated in the colour figure 10.

In both the continuous gradient and the step experiment we see that the front will form only if there is a change in the effective density gradient. Isopycnals travel at constant separation until they approach the zone of density-gradient change, where they accumulate to produce a front.

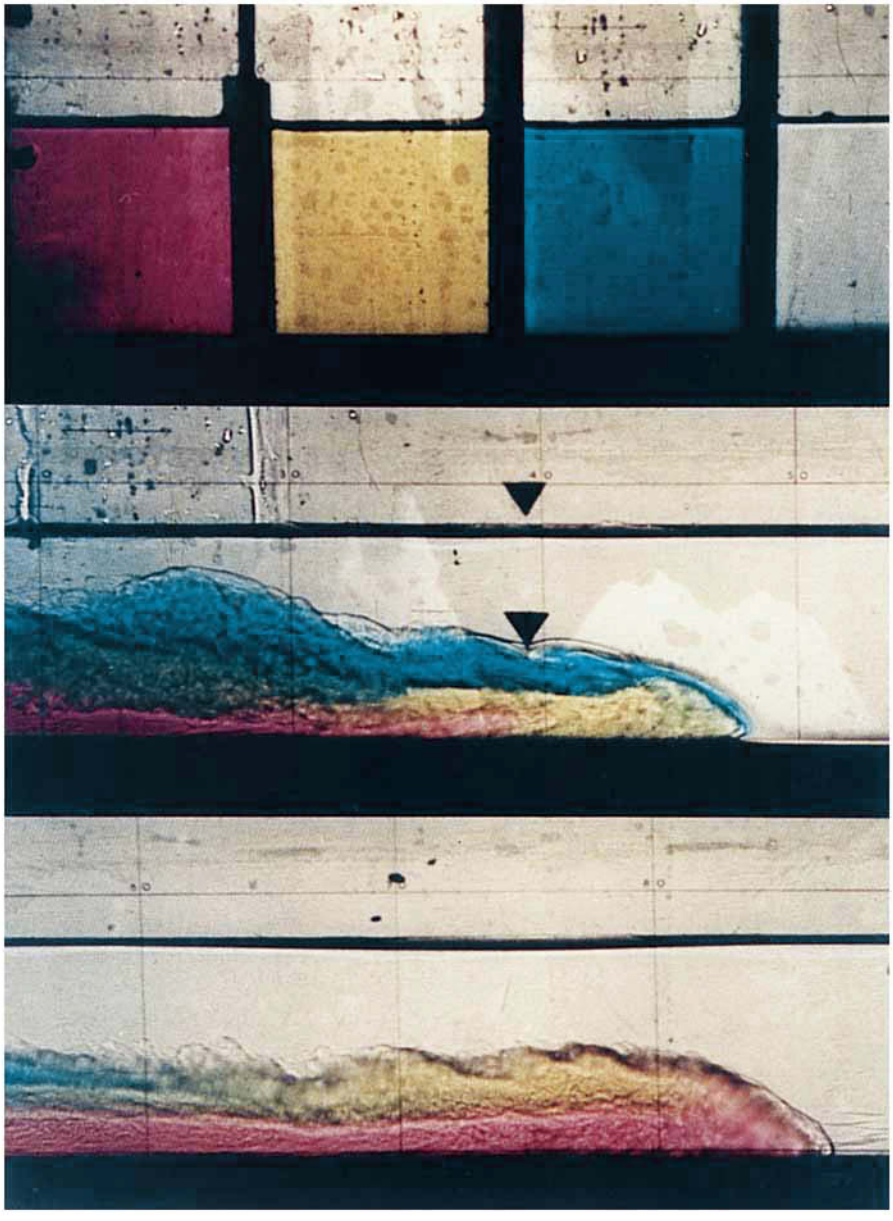

FIGURE 10. Three stages in the development of a fluid of horizontal step density profile advancing into a fluid of constant density. *(a)* The densities of the red, yellow and blue fluids are respectively 3%, 2% and 1% greater than the fresh water in the rest of the tank. *(b)* The leading edge of the yellow has caught up the blue and has formed a front there, but the distance between the leading edge of the red and that of the yellow remains the same as initially. *(c)* The red fluid has arrived at the front.

7. Discussion

The adjustment under gravity of fluid containing horizontal and vertical density gradients has been calculated and the results compared with laboratory experiments. The main conclusions are as follows.

(*a*) In a fluid with a *constant* horizontal density gradient the adjustment takes place by a continuous tilting of the isopycnals towards the horizontal. During this process the isopycnals remain straight and the horizontal density gradient remains unchanged from its initial value. The gradient Richardson number is constant in space and decreases steadily to the value $\frac{1}{2}$ at large times. This result suggests (but does not prove as the conditions for the Miles–Howard theorem are not strictly satisfied: see Drazin & Reid 1981) that the flow is linearly stable. The laboratory observations confirm these conclusions. There was no evidence of frontogenesis or internal instabilities in the flow.

(*b*) In a fluid with a non-constant horizontal density gradient, frontogenesis can occur. The presence of the initial curvature in the density field leads to a circulation in the transverse plane and the magnitude of the density gradient can increase with time. Both theory and experiment show that frontogenesis occurs on the boundary. A front is produced in a finite time and it propagates as a classical gravity current once it is fully formed. Calculations and experiments were carried out with a piecewise constant density gradient and are shown to be in agreement.

(*c*) A fluid with an initial horizontal step density profile advancing into a fluid of constant density gives a useful analogy to the non-constant continuous density gradient example.

Frontogenesis, therefore, relies on a non-uniformity in the horizontal density variation. Suppose there is a region of initial width L and depth H which contains fluid with curvature of the density field ρ_{xx} and horizontal density gradient ρ_x. The timescale τ for frontogenesis is given by (3.14) to be

$$\tau \sim c\left[\frac{g}{\bar{\rho}} L\rho_{xx}\right]^{-\frac{1}{2}},$$

where the experiment give a value of $c \approx 4$. In this time the position of the zone will have propagated a distance $h \sim H\rho_x/L\rho_{xx}$. We note that frontogenesis will only occur when the motion in the region of stronger horizontal gradient is towards the region of weaker gradient. When ρ_x is negative, as is the convention in our experiments, the front forms on the bottom of the tank when ρ_{xx} is positive and on the top when ρ_{xx} is negative.

This work was supported by a grant from the Natural Environment Research Council. We wish to thank Dr J. O'Donnell who contoured the plots shown in figures 2 and 3 and for his comments on an earlier draft of the paper. We are grateful to D. C. Cheesley, D. Lipman and J. Sharpe for their help in running the experiments.

Appendix

The advection of the density field for a piecewise constant density gradient is calculated using the small time expansion in §3. Consider the next term in the power-series expansion (3.6). At $O(t)$ we have

$$2\nabla^2\psi_2 = -\frac{g\rho_{1x}}{\bar{\rho}} = 0, \tag{A 1}$$

$$\rho_2 = +\tfrac{1}{2}[\psi_{1z}\rho_{0x} - \psi_{1x}\rho_{0z}]. \tag{A 2}$$

In order to determine the development of the density field only the last equation is needed. Substituting from (3.13), and using (3.11) we find

$$\rho = \bar{\rho}(1-\alpha_1 x) - g\bar{\rho}t^2\left(\tfrac{1}{2}\alpha_1^2 z - \frac{(\alpha_1-\alpha_2)\,\alpha_1 h}{\pi^2}\sum_{m=0}^{\infty}\frac{(-1)^m}{(2m+1)^2}\sin\frac{(2m+1)\,\pi z}{h}\right.$$
$$\left.\exp\frac{(2m+1)\,\pi x}{h}\right), \quad x<0,$$
$$= \bar{\rho}(1-\alpha_2 x) - g\bar{\rho}t^2\left(\tfrac{1}{2}\alpha_2^2 z + \tfrac{1}{2}(\alpha_1-\alpha_2)\,\alpha_2 h\sum_{m=0}^{\infty}\frac{(-1)^m}{(2m+1)^2}\sin\frac{(2m+1)\,\pi z}{h}\right.$$
$$\left.\exp-\frac{(2m+1)\,\pi x}{h}\right), \quad x>0. \tag{A 3}$$

Frontogenesis occurs when there is an increase in the horizontal density gradient ρ_x. The maximum value of the gradient occurs at $x = 0$ and from (A 3) we see that as $x \to 0^+$

$$\rho_x = -\alpha_2\bar{\rho} + \tfrac{1}{2}g\bar{\rho}t^2(\alpha_1-\alpha_2)\,\alpha_2\pi\ln\left[\tan\left(\tfrac{1}{4}\pi\left(1+\frac{2z}{h}\right)\right)\right]. \tag{A 4}$$

Since $\alpha_1 > \alpha_2$, (A 4) shows that the gradient increases with time for $z < 0$ and decreased for $z > 0$, and so frontogenesis will only occur along the bottom of the tank. This confirms the deduction made from the stream-function field and the isopycnal deformation shown in figure 3.

The horizontal density gradient increases most rapidly near $z = -\frac{1}{2}h$ when the second term in (A 4) is unbounded. The strong dependence on the vertical coordinate makes it difficult to use (A 4) to estimate the timescale for frontogenesis. We can note that the two terms in (4.16) become comparable in magnitude when

$$t = c\,[g(\alpha_1-\alpha_2)]^{-\frac{1}{2}}. \tag{A 5}$$

REFERENCES

Drazin, P. G. & Reid, W. H. 1981 *Hydrodynamic Stability*. Cambridge University Press, 525 pp.

Lamb, H. 1932 *Hydrodynamics*. Cambridge University Press, 728 pp.

Linden, P. F. & Simpson, J. E. 1986 Gravity-driven flows in a turbulent fluid. *J. Fluid Mech.* **172**, 481–497.

Milne-Thompson, L. M. 1962 *Theoretical Hydrodynamics*. Macmillan. 743 pp.

Nof, D. 1979 Generation of fronts by mixing and mutual intrusion. *J. Phys. Oceanogr.* **9**, 298–310.

Oster, G. 1965 Density gradients. *Sci. Am.* **213**, 70–76.

Simpson, J. E. 1982 Gravity currents in the laboratory, atmosphere and ocean. *Ann. Rev. Fluid Mech.* **14**, 213–234.

Simpson, J. E. & Britter, R. E. 1979 The dynamics of the head of a gravity current advancing over a horizontal surface. *J. Fluid Mech.* **94**, 477–495.